Biochemical and Biophysical Research Communications xxx (2017) 1–7

Contents lists available at ScienceDirect

Biochemical and Biophysical Research Communications

journal homepage: www.elsevier.com/locate/ybbrc

One-step construction of a molybdenum disulfide/multi-walled carbon nanotubes/polypyrrole nanocomposite biosensor for the *ex-vivo* detection of dopamine in mouse brain tissue

Kathiresan Vijayaraj [a, 1], Thirumalai Dinakaran [a, 1], Yujeong Lee [b], Suhkmann Kim [c], Hyung Sik Kim [d], Jaewon Lee [b, **], Seung-Cheol Chang [e, *]

[a] *Graduate Department of Chemical Materials, Pusan National University, Busan, 46241, Republic of Korea*
[b] *College of Pharmacy, Molecular Inflammation Research Center for Aging Intervention, Pusan National University, Busan, 46241, Republic of Korea*
[c] *Department of Chemistry, Center for Proteome Biophysics and Chemistry Institute for Functional Materials, Pusan National University, Busan, 46241, Republic of Korea*
[d] *School of Pharmacy, Sungkyunkwan University, Suwon, 16419, Republic of Korea*
[e] *Institute of BioPhysio Sensor Technology, Pusan National University, Busan, 46241, Republic of Korea*

ARTICLE INFO

Article history:
Received 27 September 2017
Accepted 12 October 2017
Available online xxx

Keywords:
Ex vivo sensor
Dopamine
Mouse Parkinson's disease model
Molybdenum disulfide
One-step electrochemical deposition

ABSTRACT

We developed a new strategy for construction of a biosensor for the neurotransmitter dopamine. The biosensor was constructed by one-step electrochemical deposition of a nanocomposite in aqueous solution at pH 7.0, consisting of molybdenum disulfide, multi-walled carbon nanotubes, and polypyrrole. A series of analytical methods was performed to investigate the surface characteristics and the improved electrocatalytic effect of the nanocomposite, including cyclic voltammetry, electrochemical impedance spectroscopy, field-emission scanning electron microscopy, atomic force microscopy, and Raman spectroscopy. The constructed biosensor showed high sensitivity (1.130 $\mu A \mu M^{-1} cm^{-2}$) with a dynamic linearity range of 25–1000 nM and a detection limit of 10 nM. Additionally, the designed sensor exhibited strong anti-interference ability and satisfactory reproducibility. The practical application of the sensor was manifested for the *ex vivo* determination of dopamine neurotransmitters using brain tissue samples of a mouse Parkinson's disease model.

1. Introduction

Dopamine (DA), a catecholamine neurotransmitter, plays a critical role in the functioning of human metabolism, and in the cardiovascular, central nervous, renal, and hormonal systems [1]. An abnormal level of DA neurotransmission is related to various neurological disorders such as Parkinson's disease (PD) [2]. Hence, the accurate determination of DA in body fluids is crucial to diagnose diseases. Various analytical studies have indicated that an electrochemical route represents one of the most attractive and suitable techniques for DA detection, and has often been utilized in clinical analyses [3]. However, the direct electrochemical detection of DA in real samples is quite limited because the electrochemical potential window of DA is close to that of numerous other biological substances in the blood, urine, or central nervous system, such as ascorbic acid (AA). To overcome this limitation, some attempts have been made to develop biosensors that could improve the selectivity with high sensitivity in DA analysis [4].

During the last decade, molybdenum disulfide (MoS_2) nanocomposites have been employed as a "next-generation nanomaterial" [5,6] for nano-electronics and electrochemical biosensors [7,8]. Currently, MoS_2 nanosheets produced by thermal methods are commercially available and several other methods have been employed for the preparation of MoS_2 nanocomposites [9]. Among these methods, electrochemical methods show great advantages in the sensor fabrication process. They are green, efficient, inexpensive, rapid, and it is easy to control the thickness of the film on the

Abbreviations: MoS_2, molybdenum disulfide; PPy, polypyrrole; PD, Parkinson's disease; MPTP, 1-methyl-4-phenyl-1,2,5,6-tetrahydropyridine; R_{ct}, charge transfer resistance; i_{pa}, anodic peak current; STR, striatum; TH, tyrosine hydroxylase.

* Corresponding author.
** Corresponding author.
E-mail addresses: neuron@pusan.ac.kr (J. Lee), s.c.chang@pusan.ac.kr (S.-C. Chang).

[1] These authors contributed equally to this work.

https://doi.org/10.1016/j.bbrc.2017.10.059
0006-291X/

electrode surface without additional treatment. However, most of the MoS_2 nanocomposites reported to date required a "multi-step" fabrication process, including a poly (xanthurenic acid)-MoS_2 film for guanine and adenine [10], MoS_2-graphene nanocomposite for folic acid in human serum [11], and gold nanoparticles-MoS_2 microcubes for microRNA-21 [12]. Carbon nanotubes (CNTs) have also been utilized in electrochemical biosensors, and multi-walled CNTs (MWCNTs) showed selective and high electrocatalytic activity toward DA [13]. However, multi-step procedures were required to cross-link the modifiers or binders, which are laborious and time-consuming. Therefore, there is an urgent need to adopt a "one-step" sensor fabrication process. To realize this approach, we hypothesized that a combined nanocomposite with MoS_2 and MWCNT could be deposited by a one-step electrochemical process for the effective determination of DA. To deposit the nanocomposite, the direct electrochemical polymerization and deposition of a biocompatible conducting polymers, polypyrrole (PPy), can be applied as a suitable one-step approach. Although PPy has been intensively employed to construct electrochemical biosensors, its electrochemical deposition has generally been carried out in highly acidic solutions [14,15].

In the present study, we developed a new one-step electrochemical deposition technique to fabricate nanocomposite DA biosensors (Fig. 2A). A homogeneous mixture solution of MoS_2, MWCNT, and pyrrole was produced and the MoS_2/MWCNT/PPy nanocomposite was electrochemically formed in aqueous solution at pH 7.0. To the best of our knowledge, this one-step electrochemical deposition procedure has never been used for a neutral solution or applied for the selective determination of DA. The proposed nanocomposite biosensor showed improved electrocatalytic activity towards DA and was successfully applied for the *ex vivo* determination of DA in the brain tissue of a mouse PD model.

2. Materials and methods

2.1. Materials and chemicals

MWCNTs (outer diameter: 6–9 nm; diameter: 5.5 nm; length: 5 μm; purity: >95%), $Na_2MoO_4 \cdot H_2O$, pyrrole monomer (Py), dopamine hydrochloride (DA), epinephrine (EP), AA, uric acid (UA), and $K_3[Fe(CN)_6]$ were purchased from Sigma Aldrich (USA). All other chemicals were of analytical grade and used as received. All aqueous solutions were prepared using deionized water (Milli-Q water purifying system, 18 MΩ cm^{-1}).

2.2. Instrumentation

Cyclic voltammetry (CV) and amperometry were carried out using a potentiostat (CompactStat, Ivium Technologies, the Netherlands) with a conventional three-electrode cell system consisting of a glassy carbon electrode (GCE; 3 mm in diameter), Ag/AgCl reference electrode, and platinum wire auxiliary electrode. Electrochemical impedance spectroscopy (EIS) was performed using an electrochemical workstation (VersaSTAT, Princeton Applied Research, USA) in the frequency range of 100 kHz to 0.1 Hz at a DC potential of 250 mV and AC potential of ±5 mV. To investigate the surface characteristics, field-emission scanning electron microscopy (FE-SEM), atomic force microscopy (AFM), and Raman spectroscopy were carried out using the sensors modified onto iridium tin oxide electrodes. SEM was performed using FE-SEM (Hitachi S-4200, Japan) operated at 15 kV, 150 W. The surface topography of the modified biosensors was characterized using AFM analysis [16]. Raman spectra were recorded on a LabRAM HR Raman spectrometer (HORIBA Scientific, France). X-ray diffraction (XRD) patterns were collected on an X-ray D/max-2200vpc (Rigaku Corporation, Japan) operated at 40 kV and 20 mA using Cu kα radiation (K = 0.15406).

2.3. Nanocomposite biosensor preparation

MoS_2 nanosheets were synthesized and treated with HNO_3/H_2SO_4 (1:1, v/v) using the method reported previously [17]. The MoS_2/MWCNT/Py suspension was prepared by mixing 10 mg of MoS_2 with 5 mg of MWCNT, which was dispersed in 14.9 mL of 1 M H_2SO_4, and then 0.1 mL of 0.05 mM pyrrole monomer solution prepared in 1 M H_2SO_4 was added to form a homogeneous brown color suspension. This mixed suspension was vigorously stirring for 60 min and then sonicated for 30 min at ambient conditions. The suspension was centrifuged for 30 min at 10,000 rpm and washed with water three times (10 min at 10,000 rpm each) to eliminate any loosely adsorbed carbon metal-containing particles and pyrrole monomers. The resulting product was redispersed into 15 mL of water to form a 1 mg/mL suspension. The MoS_2/MWCNT/Py suspension was collected and stored at 4 °C until use. A bare GCE was polished using 0.3-μm alumina slurries and sonicated in ethanol for 10 min. After sonication, the GCE was rinsed thoroughly with distilled water and dried at ambient temperature. Prior to nanocomposite deposition, an 8-μL aliquot of the suspension was drop-casted onto the surface of the GCE and dried in ambient conditions. CV was then carried out to deposit the nanocomposite by potential sweeping from −0.2 V to +0.8 V for 15 cycles at a scan rate of 50 mVs^{-1} in 0.1 M phosphate-buffered saline (PBS, pH 7.0). The constructed biosensor is denoted as GCE-MoS_2/MWCNT/PPy.

2.4. MPTP-induced PD model and immunohistochemistry

To investigate the *ex vivo* application of the biosensor, we used a well-known neurotoxin 1-methyl-4-phenyl-1, 2, 5, 6-tetrahydropyridine (MPTP)-induced PD model. MPTP was found to be a neurotoxin that can induce Parkinsonism [18]. MPTP induces the selective loss of dopaminergic neurons in the nigrostriatal pathway resulting in DA loss in striatum (STR). Male C57BL/6 mice (6 weeks old, 18–21 g) were obtained from Daehan Biolink Co. Ltd. (Chungbuk, Korea). Animals were housed under temperature- and light-controlled conditions (20–23 °C, 12-h light/dark cycle) with free access to food and drinking water. The mice were randomly divided into two groups of five mice per group (control and MPTP group) and then acclimatized for one week prior to drug administration. To induce the PD model, MPTP was administered intraperitoneally at 20 mg/kg body weight four times in one day with 2-h intervals. The mice were killed 24 h after MPTP administration, and the STR was dissected and lysed with 0.1 M PBS (pH 7.0) for DA analysis. For the control group, the same volume of 0.1 M PBS (pH 7.0) was administered intraperitoneally to the mice, and then the mice were killed, and the STR and cortex were collected and prepared for DA analysis. All samples were normalized to the same amounts of protein. For histological study, we followed the protocol described previously [19]. Briefly, mice were intracardially perfused with a 4% paraformaldehyde in 10 mM PBS. Brains were cryopreserved with 30% sucrose solution. Brains were sectioned at 40 μm in the coronal plane and immunostaining was conducted on sections containing STR or cortex with primary anti-tyrosine hydroxylase (TH, dopaminergic neuronal marker). Images were acquired using a Nikon ECLIPSE TE 200-U microscope (Nikon, Tokyo). The animal protocol used in this study was reviewed and approved by the Pusan National University-Institutional Animal Care Committee (PNU-IACUC; Approval Number PNU-2011-000330).

Please cite this article in press as: K. Vijayaraj, et al., One-step construction of a molybdenum disulfide/multi-walled carbon nanotubes/polypyrrole nanocomposite biosensor for the *ex-vivo* detection of dopamine in mouse brain tissue, Biochemical and Biophysical Research Communications (2017), https://doi.org/10.1016/j.bbrc.2017.10.059

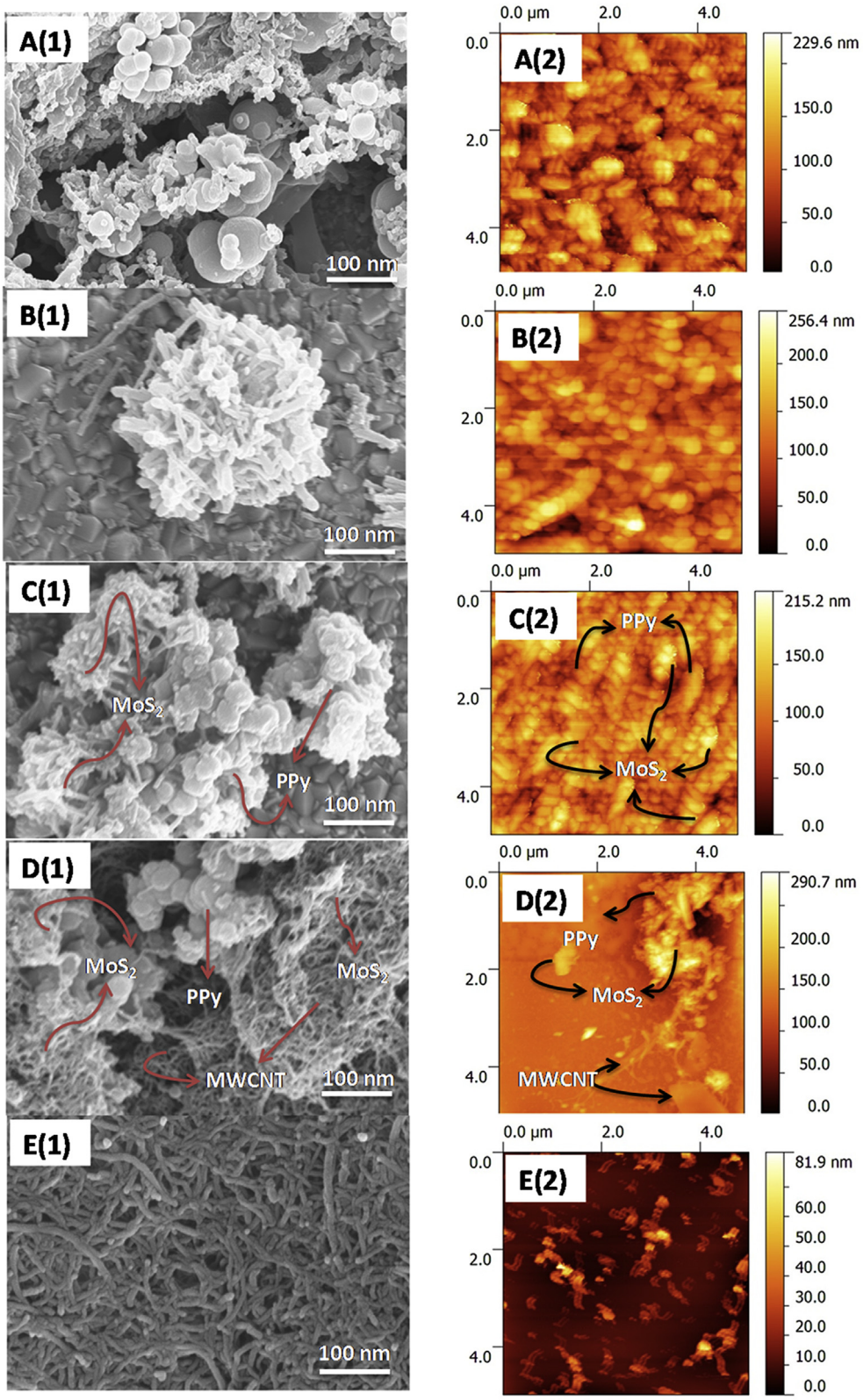

Fig. 1. FE-SEM and AFM images of (A) PPy, (B) MoS_2, (C) MoS_2/PPy, (D) MoS_2/MWCNT/PPy, and (E) MWCNT modified ITO electrodes.

3. Results and discussion

3.1. Surface characteristics of the nanocomposite electrodes

The morphological information of PPy-, MoS_2-, MoS_2/PPy-, MoS_2/MWCNT/PPy-, and MWCNT-modified surfaces was obtained using FE-SEM images. Pure PPy showed a spherical-like morphology (Fig. 1A(1)), whereas the FE-SEM image of MoS_2 nanosheets showed a flower-like morphology [20] (Fig. 1B(1)). Compared to the sole MoS_2, the electrochemically deposited MoS_2/

Please cite this article in press as: K. Vijayaraj, et al., One-step construction of a molybdenum disulfide/multi-walled carbon nanotubes/polypyrrole nanocomposite biosensor for the *ex-vivo* detection of dopamine in mouse brain tissue, Biochemical and Biophysical Research Communications (2017), https://doi.org/10.1016/j.bbrc.2017.10.059

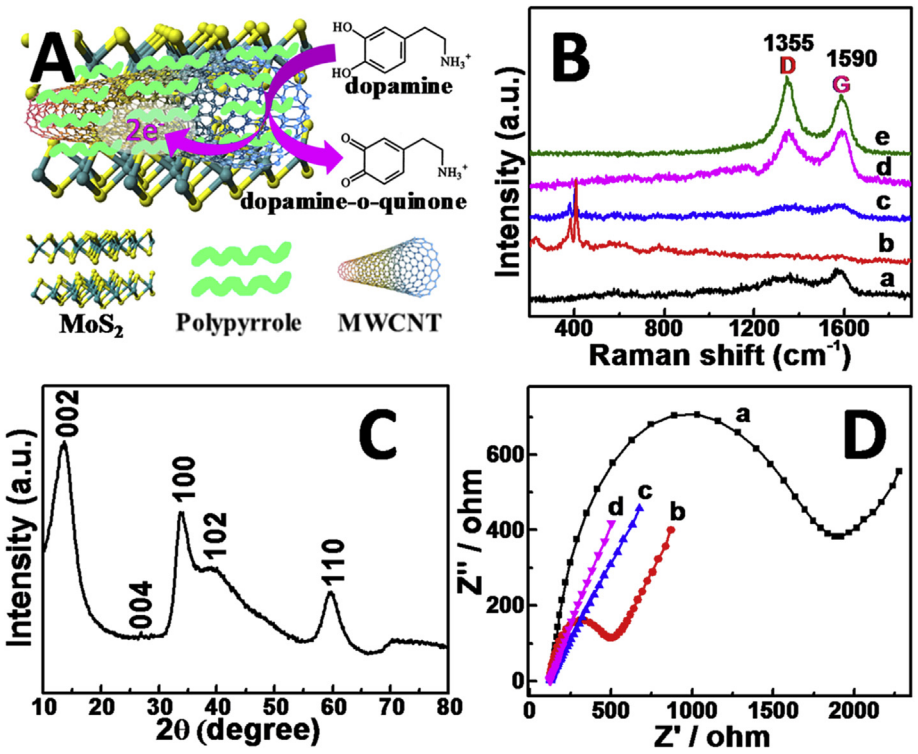

Fig. 2. A: A schematic representation of the one-step construction of MoS_2/MWCNT/PPy nanocomposite DA biosensor. **B**: Raman spectra of (a) PPy, (b) MoS_2, (c) MoS_2/PPy, (d) MoS_2/MWCNT/PPy, and (e) MWCNT surfaces. **C**: X-ray diffraction pattern of MoS_2 nanostructures. **D**: EIS of (a) GCE-PPy, (b) GCE-MoS_2, (c) GCE-MoS_2/PPy, and (d) GCE-MoS_2/MWCNT/PPy containing 5 mM $K_3Fe(CN)_6$ in 0.1 M KCl.

PPy (Fig. 1C(1)) showed both a spherical and flower-like morphology due to the electrostatic interaction between MoS_2 and PPy. When the MWCNTs were incorporated electrochemically onto the MoS_2/PPy (Fig. 1D(1)) surface, spherical, flower, and nanowire-like morphologies were observed compared to the pristine MoS_2/PPy (Fig. 1C(1)) and MWCNTs surfaces (Fig. 1E(1)), indicating synergistic effects among MoS_2, MWCNTs, and PPy. These morphological and roughness changes were confirmed by the additional AFM analysis. As shown in Fig. 1A(2), the formation of the PPy film by the electrochemical polymerization of pyrrole was confirmed by the appearance of small-sized globular particles (roughness 14.5 nm) due to the gravel-like polymer structure. The surface roughness of the MoS_2 layers was calculated to be 16.7 nm, which was greater than that obtained from only the PPy-modified layer (Fig. 1B(2)). The surface roughness of MoS_2/PPy was also calculated to be 10.7 nm (Fig. 1C(2)) and the roughness was decreased compared to that of the MoS_2-modified layers, suggesting a stronger interaction of MoS_2/PPy. Similarly, as shown in Fig. 1E(2) the only MWCNTs-modified layers showed an approximately 50% decrease of the surface roughness (6.3 nm) compared to the electrochemically deposited MoS_2/MWCNT/PPy (13.5 nm, Fig. 1D(2)). Therefore, these AFM results clearly confirmed the grain, globular, and nanowire structures of the MoS_2/MWCNT/PPy nanocomposite layers, and the successful electrochemical deposition of the nanocomposite.

The structural changes of (a) PPy, (b) MoS_2, (c) MoS_2/PPy, (d) MoS_2/MWCNT/PPy, and (e) MWCNTs were further evidenced by Raman analysis (Fig. 2B). The Raman spectrum of the electrochemically deposited PPy film showed strong peaks at 1335 cm^{-1} and 1583 cm^{-1} attributed to pyrrole-ring stretching and C=C bond stretching [21]. The Raman spectra indicated the presence of characteristic peaks of MoS_2 in the region from 200 cm^{-1} to 2000 cm^{-1} as indicated by two bands at 382 cm^{-1} and 405 cm^{-1} due to E_{2g} and A_{1g} modes [22], respectively. After the deposition of MoS_2/PPy, the peak intensity decreased remarkably (1335 cm^{-1} and 1583 cm^{-1}) compared to that of PPy alone [23]. The Raman spectrum of the MWCNTs and MoS_2/MWCNT/PPy displayed two intensive peaks at 1355 cm^{-1} and 1590 cm^{-1}, which resembled the described D and G bands. The Raman results from MoS_2/MWCNT/PPy further confirmed that the two bands at 388 cm^{-1} and at 408 cm^{-1} in the range of 350–450 cm^{-1}, can be caused by the formation of MoS_2 with comparison to the Raman spectrum of MWCNTs without distinct peaks. The intensity of Raman peaks from MWCNTs without MoS_2 (D and G bands) was remarkably higher than that from MoS_2/MWCNT/PPy. This dramatic increase could be ascribed to improvement of the defect in the concentration of MWCNTs during the electrochemical deposition of MoS_2/MWCNT/PPy [24]. XRD was performed to study the crystal structure of the MoS_2 layers. The spectra diffraction peaks at 14°, 27°, 34°, 39°, and 59° are attributed to the (002), (004), (100), (102), and (110) planes of MoS_2, respectively (Fig. 2C). These spectra also confirmed the formation of the MoS_2 layers [17].

3.2. Electrochemical characterization

3.2.1. Electrochemical impedance spectroscopy

EIS can provide important information of the impedance changes at the interface between an electrode and electrolyte [25]. Fig. 2D depicts the Nyquist diagrams of (a) GCE-PPy, (b) GCE-MoS_2, (c) GCE-MoS_2/PPy, and (d) GCE-MoS_2/MWCNT/PPy. The PPy showed an increased the charge-transfer resistance (R_{ct}) value of 242 Ω because of the poor conductivity, and the electrochemically deposited MoS_2/MWCNT/PPy showed an R_{ct} value of 29 Ω, which is smaller than that of PPy. The R_{ct} value from the MoS_2/MWCNT/PPy surface was nearly 8.3-times lower than that of PPy, and MoS_2/MWCNT/PPy had the lowest R_{ct} value compared to PPy, MoS_2, and

Please cite this article in press as: K. Vijayaraj, et al., One-step construction of a molybdenum disulfide/multi-walled carbon nanotubes/polypyrrole nanocomposite biosensor for the *ex-vivo* detection of dopamine in mouse brain tissue, Biochemical and Biophysical Research Communications (2017), https://doi.org/10.1016/j.bbrc.2017.10.059

MoS_2/PPy. These observations indicate a synergistic effect of the MoS_2/MWCNT/PPy nanocomposite, which provides better electrochemical performance through the improved electrical conductivity to accelerate interfacial electron transfer.

3.2.2. Cyclic voltammetry

As shown in Fig. 3A, CV measurements were carried out using four differently modified electrodes for 50 μM DA prepared in 0.1 M PBS (pH 7.0) at a scan rate of 50 mVs^{-1}: (a) GCE-PPy, (b) GCE-MoS_2, (c) GCE-MoS_2/PPy, and (d) GCE-MoS_2/MWCNT/PPy. PPy showed no distinct current response, and the anodic peak current (i_{pa}) of DA at MoS_2/PPy was slightly higher than that of MoS_2 alone. Moreover, for MoS_2/MWCNT/PPy, i_{pa} of DA dramatically increased (10.37 μA) compared to those of MoS_2/PPy (4.50 μA), MoS_2 (1.89 μA), and PPy (0.96 μA). A reasonable explanation for this finding is that the improved electrochemical deposition of the nanocomposites can only occur if the MWCNTs have many active sites with high electrocatalytic activity, a large effective surface area, and improved electrical conductivity [26]. CV measurements were repeated with different concentrations of DA (0–50 μM) using the GCEs-MoS_2/MWCNT/PPy sensor. The i_{pa} gradually increased with an increase in DA concentration, which was due to the electrocatalytic effect of DA (inset, Fig. 3A). This increase suggests that the nanocomposite could possess significantly improved electrocatalytic activity and a fast electron transfer rate towards the detection of DA.

3.2.3. Amperometry

To achieve optimum sensor performance conditions, the effects of applied potential, pH, and temperature were investigated. Hydrodynamic voltammograms were constructed using the GCE-MoS_2/MWCNT/PPy sensor following the addition of 250 nM DA. The maximum response of the electrodes was obtained at a potential of 0.30 V, and the signal response decreased dramatically beyond this potential. Accordingly, 0.30 V was used as the operating potential in all experiments. The optimum pH and temperature were assessed using the GCE-MoS_2/MWCNT/PPy sensor in PBS (pH 5–9) at temperatures varying from 25 °C to 40 °C with the addition of 250 nM DA at 0.30 V. The maximum response was obtained using the sensor in PBS at pH 7.0 at 25 °C. This pH and temperature were chosen as the optimal operating conditions and used in subsequent experiments. The electrocatalytic behavior of the sensor was investigated using amperometric measurements. The sensitivity of (a) GCE-PPy, (b) GCE-MoS_2, (c) GCE-MoS_2/PPy, and (d) GCE-MoS_2/MWCNT/PPy was calculated to be 0.45, 0.58, 0.71, and 1.13 μA μM^{-1} cm^{-2}, respectively (Fig. 3B). These results revealed that the simple one-step electrochemical deposition of the MoS_2/MWCNT/PPy nanocomposite demonstrated better electrochemical performance, which improved the sensitivity of the DA biosensor.

3.3. Sensor characteristics and calibration for DA

Sensor characteristics and calibration curves for DA were investigated using the GCE-MoS_2/MWCNT/PPy sensor. Fig. 3C shows a calibration curve of DA with a dynamic linear range of 25–1000 nM and with a linear regression equation of i (μA) = 79.08 C_{DA} (nM) + 0.0064 (R^2 = 0.997). Each point represents the mean value of five measurements and error bars represent one standard deviation. The limit of detection was found to be 10 nM and the sensor sensitivity was calculated to be 1.13 μA μM^{-1} cm^{-2}. Hence, the one-step deposition of the MoS_2/MWCNT/PPy nanocomposite represents a suitable strategy to construct an amperometric biosensor for DA sensing. The relative standard deviation as a measure of inter-electrode reproducibility was calculated to be 7.4%, and only a 3.5% loss of the initial sensor sensitivity was observed after 22-day storage at 4 °C. In addition, selectivity is one of the important characteristics to verify the performance of the

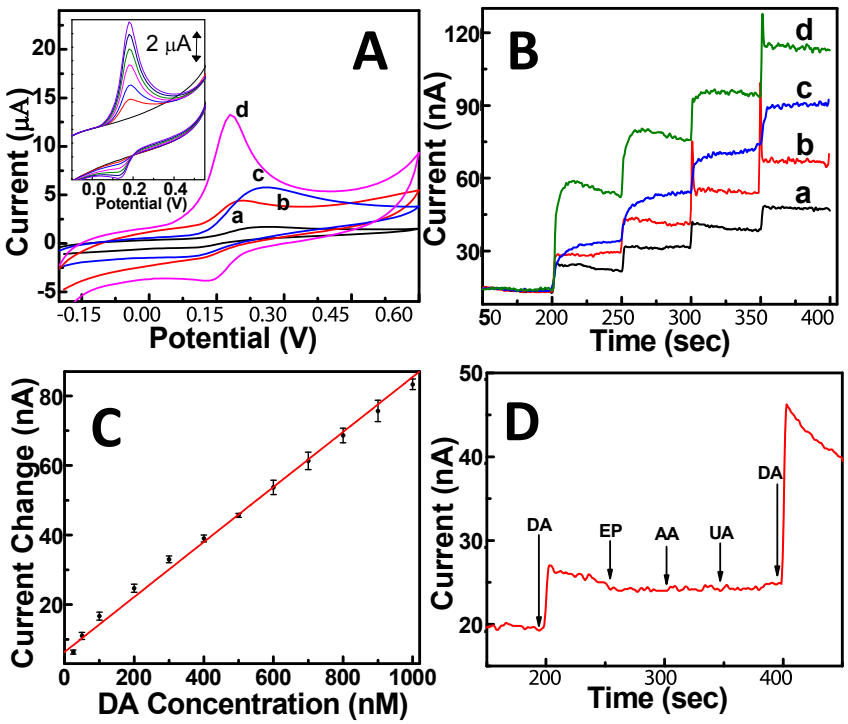

Fig. 3. **A**: CV curves of (a) GCE-PPy, (b) GCE-MoS_2, (c) GCE-MoS_2/PPy, and (d) GCE-MoS_2/MWCNT/PPy in 50 μM DA at a scan rate 50 mVs^{-1}. Inset: CV curves of GCE-MoS_2/MWCNT/PPy in DA (0–50 μM). **B**: Amperometric response of 250 nM DA on (a) GCE-PPy, (b) GCE-MoS_2, (c) GCE-MoS_2/PPy, and (d) GCE-MoS_2/MWCNT/PPy in 0.1 M PBS (pH 7.0). **C**: Calibration curve for DA using GCE-MoS_2/MWCNT/PPy in 0.1 M PBS (pH 7.0). **D**: Amperometric responses of 0.5 μM DA, 1 μM EP, 1 μM AA, 1 μM UA, and 1.0 μM DA on GCE-MoS_2/MWCNT/PPy in 0.1 M PBS (pH 7.0).

Please cite this article in press as: K. Vijayaraj, et al., One-step construction of a molybdenum disulfide/multi-walled carbon nanotubes/polypyrrole nanocomposite biosensor for the *ex-vivo* detection of dopamine in mouse brain tissue, Biochemical and Biophysical Research Communications (2017), https://doi.org/10.1016/j.bbrc.2017.10.059

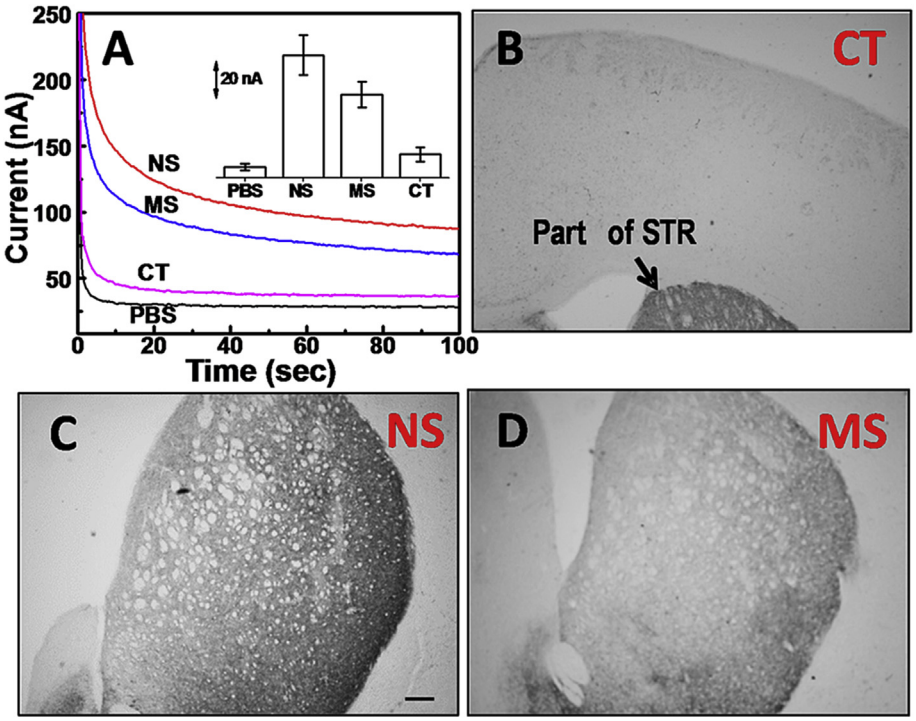

Fig. 4. **A**: Chronoamperometric response of GCE-MoS_2/MWCNT/PPy in PBS and three different mouse brain tissues: **NS** (normal STR), **MS** (MPTP damaged STR), and **CT** (cortex). Inset: each bar means *ex vivo* current change of five measurements and error bar represents one standard deviation. **B**, **C** and **D**: Images from immunestained mouse brain tissue sections, Scale bar equals 100 μm.

sensor, because real samples may also contain some potentially co-existing compounds that are common in biological systems such as DA, EP, AA, and UA. Fig. 3D shows the signal of the biosensors following the addition of 0.5 μM DA, 1 μM EP, 1 μM AA, 1 μM UA, and a second addition of 1.0 μM DA. There was no significant change in the signal in response to EP, AA, and UA, indicating no substantial interference on the detection of DA. These results indicated that the constructed biosensor exhibited enhanced electrochemical performance for DA and can be applied for *ex vivo* application.

3.4. Real sample analysis

The GCE-MoS_2/MWCNT/PPy sensor was successfully applied for real sample analysis. Three different mouse brain tissues were prepared: (NS) normal STR that receives dopaminergic inputs, (MS) MPTP damaged STR taken from the MPTP-induced PD mice, and (CT) cortical brain region lacking DA signals used as a negative control. The real samples were diluted ten times with 0.1 M PBS (pH 7.0) and chronoamperometric analysis was performed under the operating conditions. Current responses of DA were observed (Fig. 4A) and each current change was measured at 100 s. The inset in Fig. 4A represents the mean value of five measurements and error bars represent one standard deviation. The highest signal response of DA was achieved in group NS (63 ± 11 nA), followed by MS (41 ± 7 nA), CT (8 ± 4 nA), and the PBS injection control group (1 ± 2 nA). These findings demonstrate that the proposed sensor could effectively discriminate DA levels between the STR DA and cortex as DA-positive and -negative brain tissues, respectively. TH immunohistochemistry clearly indicated that TH-positive signals were only seen in STR (Fig. 4C and D) not in cortex (Fig. 4B). More interestingly, it is promising that the proposed sensor could discriminate differences of DA levels between the normal STR (Fig. 4C) and damaged STR taken from MPTP-induced PD mice (Fig. 4D), which are also observed in TH immunohistochemistry. To further test the feasibility of the MoS_2/MWCNT/PPy sensor, the mouse brain sample (NS) was diluted twenty times with 0.1 M PBS (pH 7.0), and the concentration of DA was measured using a standard addition method. The results showed very satisfactory recoveries ranging 97.6–101.6%. These observations demonstrate that the developed biosensor is a simple, fast, and reliable tool for *ex vivo* DA determination in different tissues from the brain of normal and PD model mice.

In summary, we developed an MoS_2/MWCNT/PPy nanocomposite constructed by the "one-step" electrochemical deposition procedure in aqueous solution at pH 7.0, which could be used for the determination of DA. This method was proven useful for the *ex vivo* determination of neurotransmitter DA in mouse brain tissue samples. Further research is currently underway to develop a new *ex vivo* and *in vivo* micro-sensor platform for DA determination.

Acknowledgement

This work was supported by a grant from the Pioneer Research Center Program through the National Research Foundation (NRF) funded by the Ministry of Science, ICT & Future Planning (MSIP) of Korea (2013M3C1A3065522 and 2009-0083538) and by the support of Cooperative Research Program for Agriculture Science & Technology Development (Project No. PJ011757032017) Rural Development Administration, Republic of Korea.

Transparency document

Transparency document related to this article can be found online at https://doi.org/10.1016/j.bbrc.2017.10.059.

References

[1] A. Zhang, J.L. Neumeyer, R.J. Baldessarini, Recent progress in development of

dopamine receptor subtype-selective agents: potential therapeutics for neurological and psychiatric disorders, Chem. Rev. 107 (2007) 274–302.
[2] S. Nikolaus, C. Antke, H.-W. Muller, In vivo imaging of synaptic function in the central nervous system: I. Movement disorders and dementia, Behav. Brain Res. 204 (2009) 1–31.
[3] M.-S. Hsu, Y.-L. Chen, C.-Y. Lee, H.-T. Chiu, Gold nanostructures on flexible substrates as electrochemical dopamine sensors, ACS Appl. Mater. Interfaces 4 (2012) 5570–5575.
[4] W. Wang, G. Xu, X.T. Cui, G. Sheng, X. Luo, Enhanced catalytic and dopamine sensing properties of electrochemically reduced conducting polymer nanocomposite doped with pure graphene oxide, Biosen. Bioelectron. 58 (2014) 153–156.
[5] J. Brivio, D.T.L. Alexander, A. Kis, Ripples and layers in ultrathin MoS_2 membranes, Nano Lett. 11 (2011) 5148–5153.
[6] Y. Li, C.-Y. Xu, P. Hu, L. Zhen, Carrier control of MoS_2 nanoflakes by functional self-assembled monolayers, ACS Nano 7 (2013) 7795–7804.
[7] Q.H. Wang, K. Kalantar-Zadeh, A. Kis, J.N. Coleman, M.S. Strano, Electronics and optoelectronics of two-dimensional transition metal dichalcogenides, Nat. Nanotechnol. 7 (2012) 699–712.
[8] T. Wang, R. Zhu, J. Zhuo, Z. Zhu, Y. Shao, M. Li, Direct detection of DNA below ppb level based on thionin-functionalized layered MoS_2 electrochemical sensors, Anal. Chem. 86 (2014) 12064–12069.
[9] T. Wang, H. Zhu, J. Zhuo, Z. Zhu, P. Papakonstantinou, G. Lubarsky, J. Lin, M. Li, Biosensor based on ultrasmall MoS_2 nanoparticles for electrochemical detection of H_2O_2 released by cells at the nanomolar level, Anal. Chem. 85 (2013) 10289–10295.
[10] T. Yang, M. Chen, F. Nan, L. Chen, X. Luo, K. Jiao, Enhanced electropolymerization of poly(xanthurenic acid)-MoS_2 film for specific electrocatalytic detection of guanine and adenine, J. Mater. Chem. B 3 (2015) 4884–4891.
[11] F. Chekin, F. Teodorescu, Y. Coffinier, G.-H. Pan, A. Barras, R. Boukherroub, S. Szunerits, MoS_2/reduced graphene oxide as active hybrid material for the electrochemical detection of folic acid in human serum, Biosen. Bioelectron. 85 (2016) 807–813.
[12] H.-L. Shuai, K.-J. Huang, Y.-X. Chen, L.-X. Fang, M.-P. Jia, Au nanoparticles/hollow molybdenum disulfide microcubes based biosensor for microRNA-21 detection coupled with duplex-specific nuclease and enzyme signal amplification, Biosen. Bioelectron. 89 (2017) 989–997.
[13] H. Cheng, H. Qiu, Z. Zhu, M. Li, Z. Shi, Investigation of the electrochemical behavior of dopamine at electrodes modified with ferrocene-filled double-walled carbon nanotubes, Electrochim. Acta 63 (2012) 83–88.
[14] A. Khairunnisa, W. Liao, S. Yau, Adsorption and electrochemical polymerization of pyrrole on Au (100) electrodes as examined by in situ scanning tunneling microscopy, J. Phys. Chem. C 120 (2016) 26425–26434.
[15] H. Karimi-Maleh, F. Tahernejad-Javazmi, N. Atar, M.L. Yola, V.K. Gupta, A.A. Ensafi, A novel DNA biosensor based on a pencil graphite electrode modified with polypyrrole/functionalized multiwalled carbon nanotubes for determination of 6-mercaptopurine anticancer drug, Ind. Eng. Chem. Res. 54 (2015) 3634–3639.
[16] S. Devaraju, T. Lee, A.K. Mohanty, Y.K. Hong, K.H. Yoon, Y.S. Lee, J.H. Han, H.-j. Paik, Fabrication of durable and flexible single-walled carbon nanotube transparent conductive films, RSC Adv. 7 (2017) 19267–19272.
[17] K. Krishnamoorthy, G.K. Veerasubramani, S. Radhakrishnan, S.J. Kim, Supercapacitive properties of hydrothermally synthesized sphere like MoS_2 nanostructures, Mater. Res. Bull. 50 (2014) 499–502.
[18] J.W. Langston, P.A. Ballard Jr., Parkinson's disease in a chemist working with 1-methyl-4-phenyl-1,2,5,6-tetrahydropyridine, N. Eng. J. Med. 309 (1983) 310.
[19] M.E. Kim, J.Y. Lee, K.M. Lee, H.R. Park, E. Lee, Y. Lee, J.S. Lee, J. Lee, Neuroprotective effect of bee venom is mediated by reduced astrocyte activation in a subchronic MPTP-induced model of Parkinson's disease, Arch. Pharm. Res. 39 (2016) 1160–1170.
[20] X. Zhou, B. Xu, Z. Lin, D. Shu, L. Ma, Hydrothermal synthesis of flower-like MoS_2 nanospheres for electrochemical supercapacitors, J. Nanosci. Nanotechnol. 14 (2014) 7250–7254.
[21] Y.-C. Liu, Characteristics of vibration modes of polypyrrole on surface-enhanced Raman scattering spectra, J. Electroanal. Chem. 571 (2004) 255–264.
[22] D. Gopalakrishnan, D. Damien, M.M. Shaijumon, MoS_2 quantum dot-interspersed exfoliated MoS_2 nanosheets, ACS Nano 8 (2014) 5297–5303.
[23] J. Lei, X. Lu, G. Nie, Z. Jiang, C. Wang, One-pot synthesis of algae-like MoS_2/PPy nanocomposite: a synergistic catalyst with superior peroxidase-like catalytic activity for H_2O_2 detection, Part. Part. Syst. Charact. 32 (2015) 886–892.
[24] T.N.Y. Khawula, K. Raju, P.J. Franklyn, I. Sigalas, K.I. Ozoemena, Symmetric pseudocapacitors based on molybdenum disulfide (MoS_2)-modified carbon nanospheres: correlating physicochemistry and synergistic interaction on energy storage, J. Mater. Chem. A 4 (2016) 6411–6425.
[25] B.-Y. Chang, S.-M. Park, Electrochemical impedance spectroscopy, Annu. Rev. Anal. Chem. 3 (2010) 207–229.
[26] L.A. Mercante, A. Pavinatto, L.E.O. Iwaki, V.P. Scagion, V. Zucolotto, O.N. Oliveira Jr., L.H.C. Mattoso, D.S. Correa, Electrospun polyamide 6/poly(-allylamine hydrochloride) nanofibers functionalized with carbon nanotubes for electrochemical detection of dopamine, ACS Appl. Mater. Interfaces 7 (2015) 4784–4790.

Please cite this article in press as: K. Vijayaraj, et al., One-step construction of a molybdenum disulfide/multi-walled carbon nanotubes/polypyrrole nanocomposite biosensor for the *ex-vivo* detection of dopamine in mouse brain tissue, Biochemical and Biophysical Research Communications (2017), https://doi.org/10.1016/j.bbrc.2017.10.059